Electron-Phonon Interactions in Graphene and Nanoribbons from Density Functional Theory

S.J. Aboud, M. Saraniti*, S.M. Goodnick*, M. V. Fischetti
Energy Resources Engineering, Stanford University, Stanford CA, USA
*School of Electrical, Computer and Energy Engineering Department, ASU, Tempe AZ, USA
Department of Materials Science, UT Dallas, Dallas TX, USA
e-mail: shela.aboud@stanford.edu

Graphene-based materials, particularly armchair graphene nanoribbons (AGNR), are a potentially viable option for future nano-electronics applications primarily due to the high electron mobilities measured experimentally [1]. Although much research has been done to understand how various scattering mechanisms affect the electron mobility in graphene and AGNRs [2], there are still fundamental discrepancies between experimental measurements and theory even in understanding the electron-phonon interaction governing the intrinsic mobility [3,4]. Furthermore the effective use of AGNRs in devices can be limited by a variety of sources such as edge effects, width variability, defects, and grain boundaries. In this work we use density functional theory (DFT) to calculate the electron-phonon interactions in graphene and investigate the role that structural and chemical (edges, width, and defects) variability in AGNRs influence electron transport.

The equilibrium structure and electronic dispersion of graphene and ANGRs is simulated using DFT [5] and the phonon spectra is calculated using the dynamical matrix approach [6] with forces taken from DFT. The simulated band-structure and phonon spectra are shown for graphene in Fig. 1.

Large variations in the acoustic and optical deformation potentials have been reported in literature making it difficult to accurately predict the intrinsic mobility in graphene. In this work, the DFT formalism is used in a manner similar to [7] to compute the electron-phonon matrix elements over the entire Brillouin zone (without using deformation potentials).

(1)

where the perturbation of the electronic states due to the phonons is computed directly with the derivative of the Kohn-Sham potential with respect to the atomic displacement along the direction normal with a given phonon. The scattering rates computed with the electron-phonon matrix elements will then used in a previously validated fullband Cellular Monte Carlo (CMC) code [8] to model electron transport.

The bandgap of AGNRs scale with the ribbon width and number of atomic layers due to Clar resonance structures (Clar sextets [9]) that become increasingly localized by the formation of edge states. Fig. 2 shows a plot of the DFT-based calculations of STM images of the valence band states using the Tersoff-Hamann model [10] for 9-, 10-, and 11-AGNR. The spatial localization of the Clar sextets that give rise to the trends in the bandgap as a function of ribbon width, shown in Fig. 2 (d) for both DFT (and emprical pseudopotential calculations [11]) can clearly be seen. The addition of defects, dopants and support material interactions will influence the aromicity of the π-electrons in the AGNRs further and modify the electronic structure. Phonon modes are also sensitive to the structural changes in AGNRs. In particular previous DFT calculation on the splitting of the LO-TO modes at the Γ-point in AGNRs have been shown to follow the same trends in bandgap, with the largest and smallest splitting found for ribbons with 3N+1 and 3N+2 atomic layers, respectively [12]. The phonon density-of- states for bulk, 3-AGNR, 4-AGNR and 5-AGNR are shown in Fig. 3. Our results predict that only the LO mode is dependent on the Clar structure while the TO mode just scales with width.

REFERENCES

[1] K. I. Bolotin, K. J. Sikes, J. Hone, H. L. Stormer, and P. Kim, *Temperature-dependent transport in suspended graphene*, Phys. Rev. Lett. **101**, 096802 (2008).

[2] R. S. Shishir and D. K. Ferry, *Velocity saturation in intrinsic graphene*, J. Phys.: Condens. Matter **21** 344201 (2009); K. M. Borysenko, J. T. Mullen, E. A. Barry, S. Paul, Y. G. Semenov, J. M. Zavada, M. Buongiorno Nardelli, K. W. Kim, *First-principles analysis of electron-phonon interactions in graphene*, Phys. Rev. B **81** 121412 (2010).

[3] J.-H. Chen, C. Jang, M. Ishigami, S. Xiao, E. D. Williams, and M. S. Fuhrer, *Diffusive charge transport in graphene*, Solid State Commun. **149**, 1080 (2009).

[4] V. Barone, O. Hod, G. E. Scuseria, *Electronic structure and stability of semiconducting graphene nanoribbons*, Nano Lett. **6**, 2748 (2006)

[5] The DFT calculations are carried out with the projector augmented wave (PAW) method with the exchange-correlation functions are represented with the PBE model of the generalized gradient approximation (GGA).

[6] Phonon spectra calculations for the AGNR are computed using: D. Alfe, *PHON: A program to calculate phonons using the small displacement method*, Comp. Phys. Comm., **180**, 2622 (2009).

[7] S. Piscanec, M. Lazzeri, F. Mauri, A. C. Ferrari, J. Robertson, *Kohn anomalies and electron-phonon interactions in graphite*. Phys. Rev. Lett., **93**, 185503 (2004).

[8] M. Saraniti and S. M. Goodnick, *Hybrid fullband cellular automaton/Monte Carlo approach for fast simulation of charge transport in semiconductors*, Trans. Elec. Dev., **47**, 1909 (2000).

[9] E. Clar, The Aromatic Sextet; Wiley: London 1972.

[10] J. Tersoff and D. R. Hamann, *Theory and application for the scanning tunneling microscope*, Phys. Rev. Lett. **50**, 1998 (1983).

[11] M. V. Fischetti and S. Narayanan, An empirical pseudopotential approach to surface and line-edge roughness scattering in nanostructures: Application to Si thin films and nanowires and graphene nanoribbons, J. Appl. Phys. **110**, 083713 (2011).

[12] R. Gillen, M. Mohr, C. Thomsen, J. Maultzsch, *Vibrational propoerties of graphene nanoribbons by first-priciples calculations*, Phys. Rev. B. **80**, 155418 (2009).

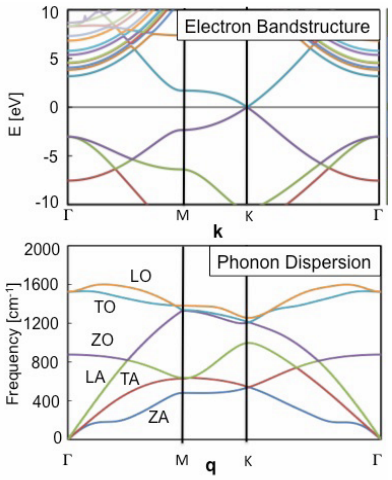

Fig. 1. Graphene bandstructure and phonon dispersion calculated with DFT and dynamical matrix method.

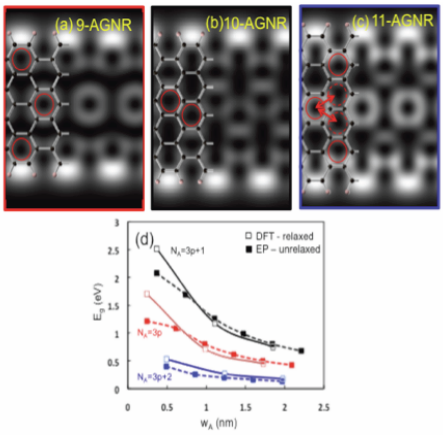

Fig. 2. (a)-(c) DFT calculated STM images of the occupied electronic states of a 9-, 10-, and 11-AGNR, respectively and (d) the trends in the electronic gap (for both DFT and EPs).

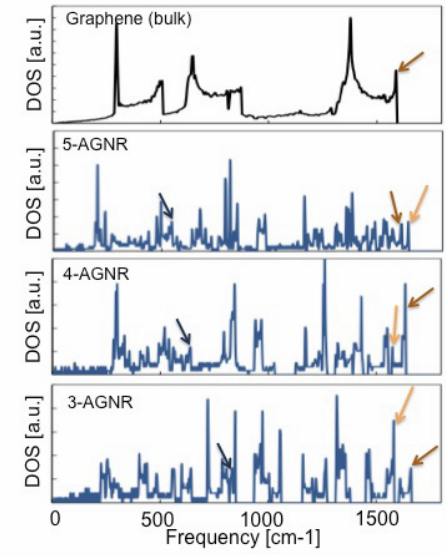

Fig. 3. Phonon density of states. The RBM is signified with the green arrow, and the LO and TO modes are signified with the dark brown and yellow arrows, respectively.